WETTING-INDUCED COLLAPSE OF CRUSHED SEDIMENTARY ROCKS UNDER HIGH STRESS

Mehrdad Ahmadi[1,2], Stephen Fityus[1,3], Klaus Thoeni[1], Ross Seedsman[4], Anna Giacomini[1] and Olivier Buzzi[1]
[1]The University of Newcastle, Australia, [2]Rain Consulting Pty Ltd, Australia, [3]Douglas Partners Pty Ltd, Australia
[4]Byrnes Geotechnical Pty Ltd, Australia

https://doi.org/10.56295/AGJ6037

ABSTRACT

This study investigates the evolution of the porosity of crushed sedimentary rock masses in one-dimensional compression for dry and inundated conditions with wetting-induced collapse at different stress levels in the context of underground pumped hydro energy storage (UPHES) facilities, where the collapsed underground void of a disused mine serves as the lower reservoir. Three fine-grained rock lithologies typically present in underground mine roofs, indurated mudstone, interbedded sandstone-mudstone, and massive siltstone with unconfined compressive strength (UCS) values in the range of 25 to 157 MPa, were subjected to constant strain rate compression tests up to a stress of 12 MPa, with different specimens of each lithology inundated at stresses of 50 kPa, 2 MPa, 5 MPa or 12 MPa. The results show that the weaker the rock, the greater the reduction in porosity under stress. The porosity reduction upon collapse is independent of the magnitude of the applied stress for the stress range considered in the tests, but its magnitude depends on the material. It is also observed that the porosity of the crushed rock samples in dry conditions under the maximum stress level (i.e., 12 MPa) increases linearly with the UCS on a semi-logarithmic scale. The stress-strain curves were scaled to account for the size of the rock boulders forming a real goaf, which is usually found in disused underground mines. It was found that the change in porosity upon collapse is not scale-dependent and, hence, can be satisfactorily characterised at the laboratory scale, provided that the particle size distribution is adequate.

1 INTRODUCTION

Sedimentary rocks are encountered in many civil and mining contexts. Even within fine-grained sedimentary rocks, strength, compressibility and response to wetting can vary over an order of magnitude, from uncemented rocks to indurated, silicious cherts. It is important to understand the behaviour of rubblised sedimentary rock masses under compressive loads since they are relevant in various engineering applications. Coarse, broken rock (rockfill) is used in the construction of earth dams and reservoirs (Oldecop and Alonso 2001; Hunter and Fell 2003). Blasted waste rock is produced as a result of open-pit mining (Bagde et al. 2002; Fityus et al. 2008; Jain et al. 2021; Salmi and Sellers 2021). Waste rock fills in rehabilitated open-pit mines may be used for commercial or industrial development, and the response of these materials to external loads in dry and wet conditions determines the serviceability of structures built on them (Karem et al. 2007). Broken rock masses are also produced during longwall coal mining (Liu et al. 2020; Zhang et al. 2022), whereby the unsupported roof collapses forming a caving zone of gob or goaf (Karacan 2010a; Zhang et al. 2022). The properties of the goaf impact gas emission, mine ventilation, water inflow, and surface subsidence.

A key element in the transition from electricity generated on demand from fossil fuels to electricity generated from renewable sources when they are available is reliable infrastructure to "bank" power when it is in surplus and release it when it is in demand. Pumped hydro systems are currently one of the few reliable options available to meet this need, and large porous underground spaces such as goaf rock have great potential for use in underground pumped hydro energy storage (UPHES) facilities (Fan et al. 2020; Jiang et al. 2021). Figure 1 shows an example of goaf material from an underground coal mine that can potentially be used as underground reservoir. The evolution of porosity in rubblised rock masses such as goaf and mine spoils is controlled by several factors including stress condition (Li et al. 2018, 2019b), rock lithology and strength (Pappas and Mark 1993; Yu et al. 2016; Li et al. 2019c), the particle size and size distribution (Ma et al. 2016; Xu et al. 2021) and the degree of saturation of the material (Yu et al. 2016).

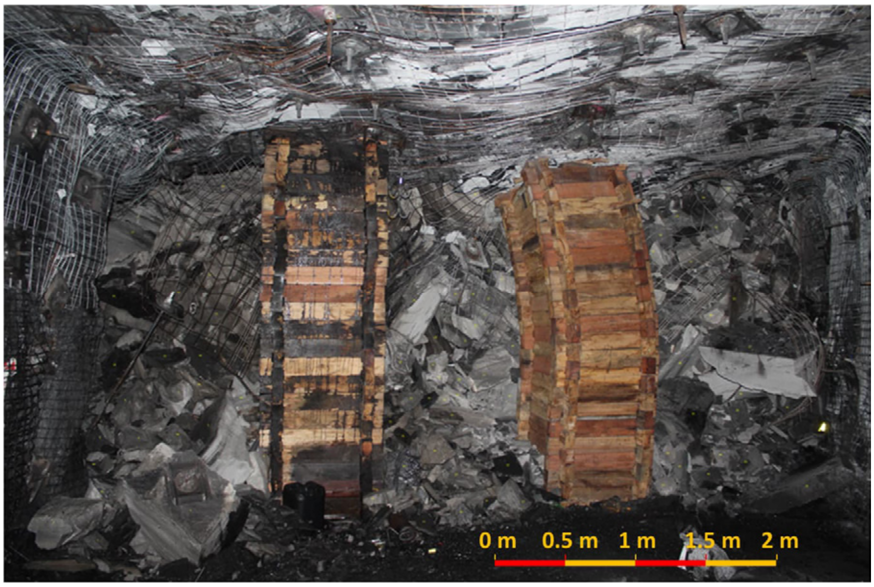

Figure 1 Image of goaf from an underground coal mine in New South Wales, Australia.

Yu et al. (2016) evaluated the influence of axial compression on saturated crushed gangue, mudstone, sandstone and limestone and showed that a strong correlation exists between porosity under a given stress and unconfined compressive strength (UCS). Li et al. (2019c) studied the effect of lateral and axial compression on crushed rock samples with different four lithologies using cyclic loading tests and observed that the sample of stronger rock lithology had a higher porosity and experienced a lower degree of crushing under a given stress.

To study the impact of the particle size distribution (PSD) on the behaviour of crushed rock under compression, Li et al. (2016) investigated the compression characteristics of sandstone with different particle size distributions, from mono-sized to poly-disperse gradations. The authors observed that poly-disperse graded specimens are less deformable than mono-sized specimens. Li et al. (2019b) also investigated the influence of particle size (i.e., 0-10 mm, 10-20 mm, 20-30 mm and 0-30 mm) on the compressive behaviour of crushed sandstone. The authors observed that the reduction of porosity is controlled by the initial porosity and that the larger the particle size, the lower the axial porosity under high axial stress levels (i.e., ~20 MPa).

Of particular interest for this study is the phenomenon of wetting-induced collapse of crushed rocks, since in UPHES facilities, water circulates between a lower and upper reservoir and the porosity of the lower reservoir, filled with goaf, affects the rate at which the reservoir can be filled and emptied. Wang et al. (2020) investigated hazards imposed by the groundwater inrush in underground deep mining operations and concluded that particle migration and mass loss lead to significant changes in the porosity of crushed rock. Oldecop and Alonso (2001) investigated the effect of saturation and relative humidity on the collapse of slate with particle sizes in a range of 1 mm to 40 mm under relatively low values of stress (less than 1 MPa) and in one-dimensional (1D) compression. The authors concluded that intra-particle suction and water adsorbed by rock particles were the controlling factors and that the intergranular suction in unsaturated rock particles in a high-humidity environment can be effectively reduced to near zero, even for low total water contents. That is, the water content stored inside larger voids, in between particles, does not contribute to the response of the rockfill material. Results of their study also suggest that the stress-strain relationship of material under stress values of less than 1 MPa either follows dry or saturated responses regardless of the saturation stress. This means that the amount of collapse due to saturation is equal to the axial strain difference between materials loaded under saturated and dry conditions in stress levels investigated by Oldecop and Alonso (2001). This finding was not corroborated by Zhou et al. (2020) who investigated the influence of saturation-induced collapse of crushed weathered granite under triaxial conditions. Triaxial tests were conducted with particle sizes in the range of 0.05 mm to 60 mm and under confining pressures and deviatoric stresses ranging from 0.2 to 1.2 MPa and 1 to 4.3 MPa, respectively. The authors observed that under the same confining stress, the sample experienced a larger amount of collapse as the deviatoric stress increased and that the amount of collapse due to saturation was higher than the overall strain difference between dry and wet conditions. However, the stress-strain responses of saturated samples converge when the deviatoric stress increases.

In their study, Tabibnejad et al. (2015) showed that the volumetric strain due to collapse does not vary significantly with particle size (ranging from 19.1 mm to 150 mm) but is affected by fine content and initial dry density. In conclusion, many studies have shown that the magnitude of wetting-induced collapse is controlled by the stress condition, initial void ratio (or density), rock type and particle size distribution (Neves and Pinto 1988). Most of these studies have focused on rockfill for dams for which the stress levels are low to moderate and the particle size is typically less than 200 mm. When dealing with a UPHES facility using a disused mine void in which goaf is present, the rock block size is much larger (see Figure 1) and so is the stress (in Australia up to 12 MPa).

This paper investigates the compression behaviour of dry and inundated crushed rock materials under a wide range of axial stresses (0-12 MPa). The results of down-scaled laboratory experiments will be used to predict the stress-strain relationship of goaf in dry and inundated conditions. The study focuses on fine-grained sedimentary rocks of different lithologies including indurated mudstone, interbedded sandstone-mudstone and massive siltstone, with particle strengths (characterised by UCS values) ranging from 42 to 157 MPa. The 12 MPa upper limit for the axial stress is equivalent to an overburden stress at a depth of 500 m (for a dry density of 2400 kg/m^3) which is around the maximum practical depth for longwall coal mining in Australia. The stress range considered in this paper is significantly higher compared to other available studies in the literature (i.e., typically less than 5 MPa) with a focus on wetting-induced collapse of crushed rock and rockfill material. Finally, considerations of scaling the laboratory-scale results are given to try and estimate the magnitude of collapse of the real-scale goaf material.

2 MATERIALS AND EXPERIMENTAL METHODS

2.1 ROCK TYPES AND PROPERTIES

Three fresh sedimentary rocks were selected for this study, with different clay contents and degrees of diagenesis, with a wide range of rock material strengths. These included an indurated mudstone of Proterozoic age from an open-pit copper/gold mine, and three Permian-aged coal measures rocks comprising: an interbedded sandstone-mudstone (2/3 sandstone and 1/3 mudstone) from an underground coal mine and a massive siltstone (non-fissile but showing indistinct laminations) from an open-pit mine. The compressive strength of the materials was determined using UCS tests on specimens cored from blocks that were retrieved from the various sites (see Figure 2). The indurated mudstone specimens were wet-cored since this lithology is the only moisture-insensitive material considered in this study. The specimens of sandstone and mudstone from the interbedded sandstone-mudstone and the massive siltstone were dry-cored since these lithologies are moisture sensitive. Due to their friability, cylindrical specimens of the mudstone from the interbedded sandstone-mudstone were firstly hand-cut to create polygonal prisms using a dry diamond saw, and then rounded to cylinders using a wood-working disc sander. The volume and mass of the air-dried cores were used in determining the rock density. The specimens to be tested in compression had a length-to-diameter ratio of 2-3 and their ends were prepared according to the ISRM recommended method (ISRM 1979). UCS tests were conducted according to AS 4133.4.2.2 (Standards Australia 2013) and AS 4133.4.3.1 (Standards Australia 2009). Values of UCS, rock densities and Weibull modulus are listed in Table 1. The UCS and point load test data were used in the calculation of the Weibull modulus. The Weibull modulus characterises the variability of the material. More details about the Weibull modulus of lithologies tested in this study are provided in Appendix A.

Table 1 UCS and rock density values for materials used in this study.

<table>
<tr><th>Material</th><th colspan="2">UCS [MPa]</th><th colspan="2">Rock Density [kg/m^3]</th><th colspan="2">Weibull modulus</th></tr>
<tr><td>Indurated mudstone</td><td colspan="2">Mean: 157
Standard deviation (SD): 63
Range: 92 – 258</td><td colspan="2">Mean: 2800
SD: 5
Range: 2790 – 2810</td><td colspan="2">2.68</td></tr>
<tr><td rowspan="3">Interbedded sandstone-mudstone</td><td>Sandstone</td><td>Mudstone</td><td>Sandstone</td><td>Mudstone</td><td>Sandstone</td><td>Mudstone</td></tr>
<tr><td>Mean: 96
SD: 53
Range: 20 – 215</td><td>Mean: 25
SD: 10
Range: 13 – 46</td><td>Mean: 2550
SD: 49
Range: 2460 – 2620</td><td>Mean:2540
SD: 60
Range: 2390 – 2580</td><td>2.11</td><td>2.95</td></tr>
<tr><td colspan="2">Weighted average: 73</td><td colspan="2">Weighted average: 2550</td><td colspan="2">Weighted average: 2.39</td></tr>
<tr><td>Massive siltstone</td><td colspan="2">Mean: 42
SD: 7
Range: 29 – 54</td><td colspan="2">Mean:2350
SD: 89
Range: 2260 – 2480</td><td colspan="2">1.96</td></tr>
</table>

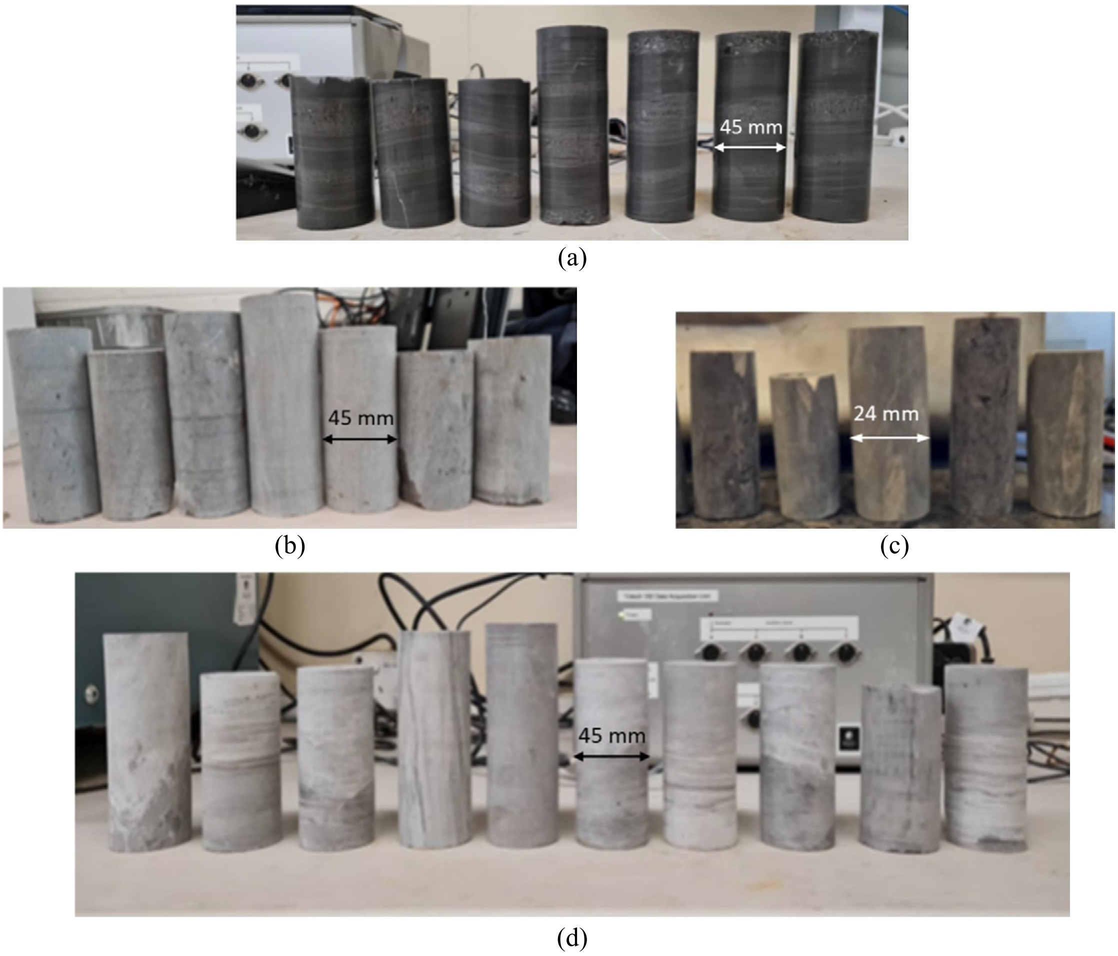

Figure 2 Specimens used for the UCS testing: (a) indurated mudstone (wet cored), (b) sandstone (dry cored) samples of interbedded sandstone-mudstone, (c) mudstone (dry cut and rounded) samples of interbedded sandstone-mudstone, and (d) massive siltstone (dry cored).

2.2 EXPERIMENTAL PROGRAM

A total of four one-dimensional (1D) compression tests were conducted on each lithology. Each 1D compression test comprises three stages, where stage one starts with the dry compression with a constant loading rate until the inundation stress is reached. Then, the specimen gets inundated under the constant stress in stage two, and finally, the compression with a constant loading rate presumes until the maximum stress of 12 MPa is achieved. A constant rate of 1 mm/min was selected to ensure quasi-static loading conditions. The difference between compression tests of the same rock lithology is the applied inundation stress, which is either 56 kPa, 2 MPa, 5 MPa, or 12 MPa. The initial porosities of specimens are presented in Table 2. Sample preparation and the testing procedure for the series of 1D compression tests are explained in Sections 2.3 and 2.4.1. To explore the scaling effect on the collapse of material due to inundation, narrow particle size distributions of 19-26 mm and 150-200 mm were used for dry compression tests. The testing procedure is explained in Section 2.4.2.

Table 2 Initial porosity of specimens

Material	Porosity of specimen
Indurated mudstone	0.51
Interbedded sandstone-mudstone	0.50
Massive siltstone	0.49

2.3 PREPARATION OF GRANULAR SPECIMENS FOR 1D COMPRESSION

To prepare specimens for the 1D compression tests, bore cores and/or lumps of materials (of similar size to the bore cores) of each lithology were crushed in a jaw crusher to produce a material with a top size of 26.5 mm. For the interbedded sandstone-mudstone, which is comprised of 2/3 sandstone and 1/3 mudstone, fresh 63 mm diameter borehole cores were available, whilst for the other lithologies, lumps were retrieved from loads of freshly excavated mine spoil. To increase similarity in the characteristics of the crushed product, the lumps of indurated mudstone and massive siltstone rock that were crushed were chosen to have a similar volume and cross-section as the pieces of drilled cores of interbedded sandstone-mudstone. As the initial particle size distribution (PSD) used in this test was arbitrary, it was decided that the PSD of all samples should be that of the naturally resulting PSD from the jaw crushing of cores/lumps, without adjustment or modification.

The PSD analyses of the various materials in Figure 3 show that the jaw crusher produces very similar PSD for the different rock lithologies when the core segments and lumps fed into the crusher have similar overall sizes.

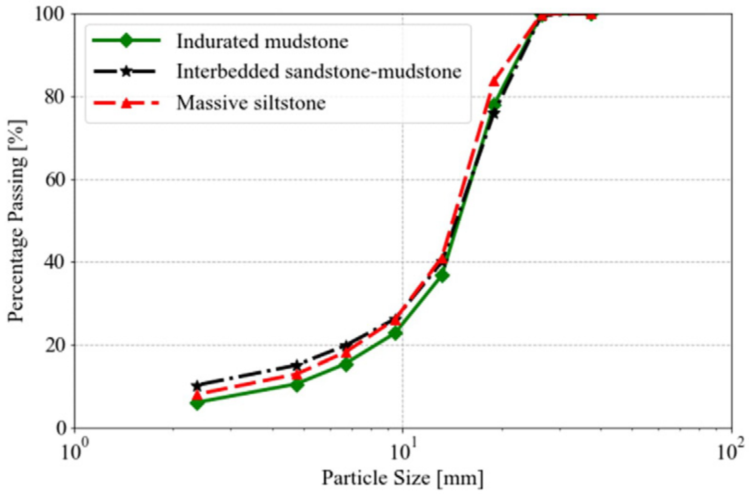

Figure 3 Particle size distribution of crushed blocks of indurated mudstone, interbedded sandstone-mudstone, and massive siltstone.

To standardise the initial conditions for each test, all specimens were prepared by loose-packing with the aim of achieving the same initial porosity. Accounting for the different specific gravity of the particles, each compression test required between 21 and 24 kg of material, so to prepare enough material for four tests on each lithology, 130 kg of the crushed rock was initially prepared. Then, five identical specimens were prepared from the bulk crushed sample using a riffle box sample splitter. One specimen was used for the PSD analysis and the four remaining specimens were used for the compression tests of that specific material.

The oedometric compression tests were carried out using a stiff cylinder ring according to the procedure described in Section 2.4.1. The ring, shown in Figure 4, has a height of 250 mm, an internal diameter of 300 mm and a wall thickness of 25 mm. It has a fixed rigid base with a grid of holes and radial grooves to allow access for water to the sample from the bottom. It should be noted that a circular piece of geofabric cloth is placed over the base (Figure 5a) before pouring the material into the ring to prevent holes from getting blocked by fine particles.

(a) (b)

Figure 4 Stiff ring used for oedometric compression tests: (a) top view, and (b) bottom view with a grid of holes in the centre, with radial grooves across the outer ring, allowing water to access the sample from the bottom.

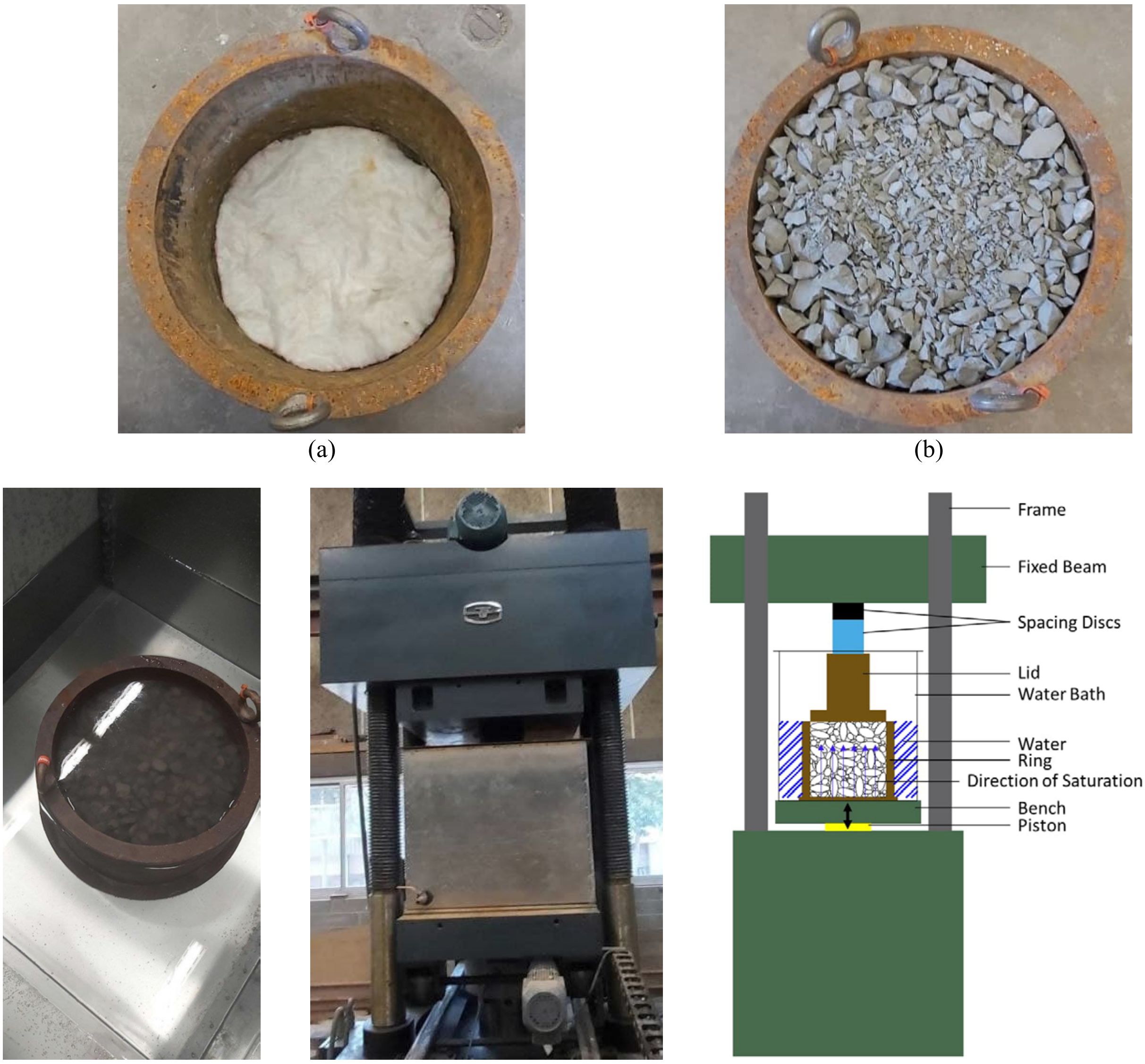

Figure 5 Compression test setup: (a) base of the ring covered with a piece of geofabric cloth to avoid loss of fine particles, (b) loose sample in the ring before the compression test, (c) inundated sample in the waterproof bath, (d) compression test machine, and (e) schematic of the test setup.

For each compression test, the crushed rock was placed loosely in the ring (Figure 5b). The ring, with the loosely packed specimen, was then carefully placed in an unfilled water bath and installed into the large compression testing machine shown in Figure 5d for the test. At some point during each test (see Section 2.4), the water bath was filled up to just below the top of the sample ring (Figure 5c), so water could only enter the ring through the perforated base. For this inundation step, the specimens were left in this arrangement for a long enough time, until water appeared at the surface of the sample inside the ring to allow the whole specimen to be inundated. The schematic of the test setup including the compression testing machine, water container, steel ring and lid, spacing discs and crushed rock sample, is shown in Figure 5e.

2.4 TESTING PROCEDURE

2.4.1 1D compression tests with wetting-induced collapse

The compression tests were carried out in three stages. To explain these stages, the evolution of settlement (black) and stress (red) versus time for the massive siltstone as an example of 1D compression test results are shown in Figure 6. The three stages are visible with a linear increase in displacement with time at the beginning and the end of the test and a stage of constant stress in between.

- Stage 1 is a dry compression at a constant rate of 1 mm/min until a target stress (2 MPa in Figure 6) is reached, at which inundation will occur (also referred to as the inundation stress).

- Stage 2 involves dry compression under constant target stress until the strain rate in the specimen falls below 0.1% per minute, followed by inundation. The initial part of Stage 2 is denoted as dry creeping in Figure 8. The specimen was inundated under constant load (i.e., the maintained inundation stress). It was noted that wetting-induced collapse began almost immediately and progressed for a considerable period before water appeared at the surface of the sample (i.e. collapse part in Figure 8). The collapse settlement slowed significantly when water appeared, and Stage 2 was maintained until the strain rate in the specimen fell below 0.1% per minute (inundated creeping part in Figure 8), at which point Stage 3 is initiated. These sub-parts are evident in Figure 8 between stages 1 and 3. Similar trends were observed for all materials. However, despite continuing Stage 2 until reaching a strain rate of lower than 0.1%, in some cases of specimens under higher inundation stresses, small, isolated pockets of dry material were observed in the sample when it was removed at the end of the test. To resolve this issue, depending on the rock strength, the sample was kept inundated under constant load for 3 hours to 4 days before Stage 3 started.
- Stage 3 is a constant strain rate compression, similar to Stage 1, where the now inundated specimen is compressed at a rate of 1 mm/min until a stress of 12 MPa is applied. Then, the test is terminated.

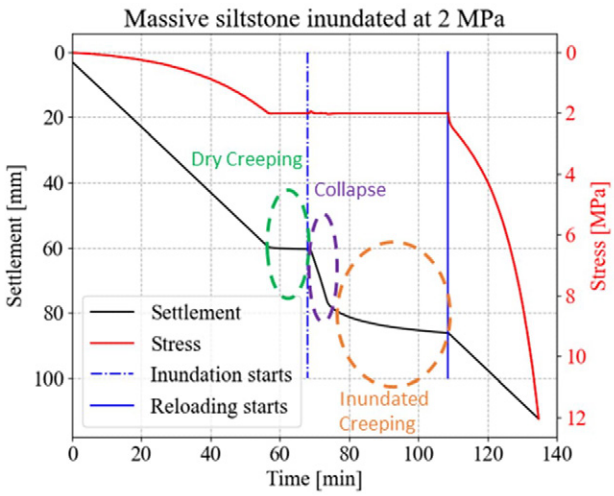

Figure 6 Evolution of settlement and stress vs. time for the massive siltstone inundated at 2 MPa

2.4.2 1D Compression tests on different particle sizes

Two dry compression tests were conducted on crushed massive siltstone to identify a possible effect of particle size on the stress-strain curve in 1D compression. A different steel ring (height of 475 mm, internal diameter of 560 mm, wall thickness of 30 mm) was used for those tests. HDPE sheets were used to line the interior of the ring to reduce the wall friction for dry tests. Figure 7 shows the two samples used for the compression tests. The particle sizes used in the two tests were in the range of 19-26 mm and 150-200 mm, respectively. The larger-size particles were carefully placed into the ring by hand to achieve a similar porosity as for the smaller-size particles. A 25 mm thick cap plate was used to transmit load to the sample, and the loading was applied at a rate of 1 mm/minute.

(a) (b)

Figure 7 Dry sample of massive siltstone used for scaling effect compression tests. a) 19-26 mm, b) 150-200 mm

3 RESULTS

Results of the three series of oedometric compression tests are presented in this section. Figure 9 shows the evolution of porosity vs. stress for all specimens and the first observation is that all specimens, from the strongest rock to the weakest, underwent some collapse. The overall trends for all rock lithologies are similar. The compression lines for the fully dry (i.e., sample inundated at 12 MPa) and fully inundated (i.e., sample inundated at 56 kPa) samples are approximately parallel, offset from each other by an approximately fixed distance for stresses greater than about 2 MPa. Where inundation was imposed at 2 MPa and 5 MPa, the wetting-induced collapse was of a similar amount and occurred such that the collapse paths followed the fully dry curve before inundation and the fully inundated curve post inundation, which is consistent with observations by Oldecop and Alonso (2001). Because the dry and inundated curves run approximately parallel, the amount of wetting-induced collapse is roughly constant for inundation at any stress greater than about 2 MPa. The change in porosity is governed by the relative position of fully dry or fully inundated responses, regardless of the target stress.

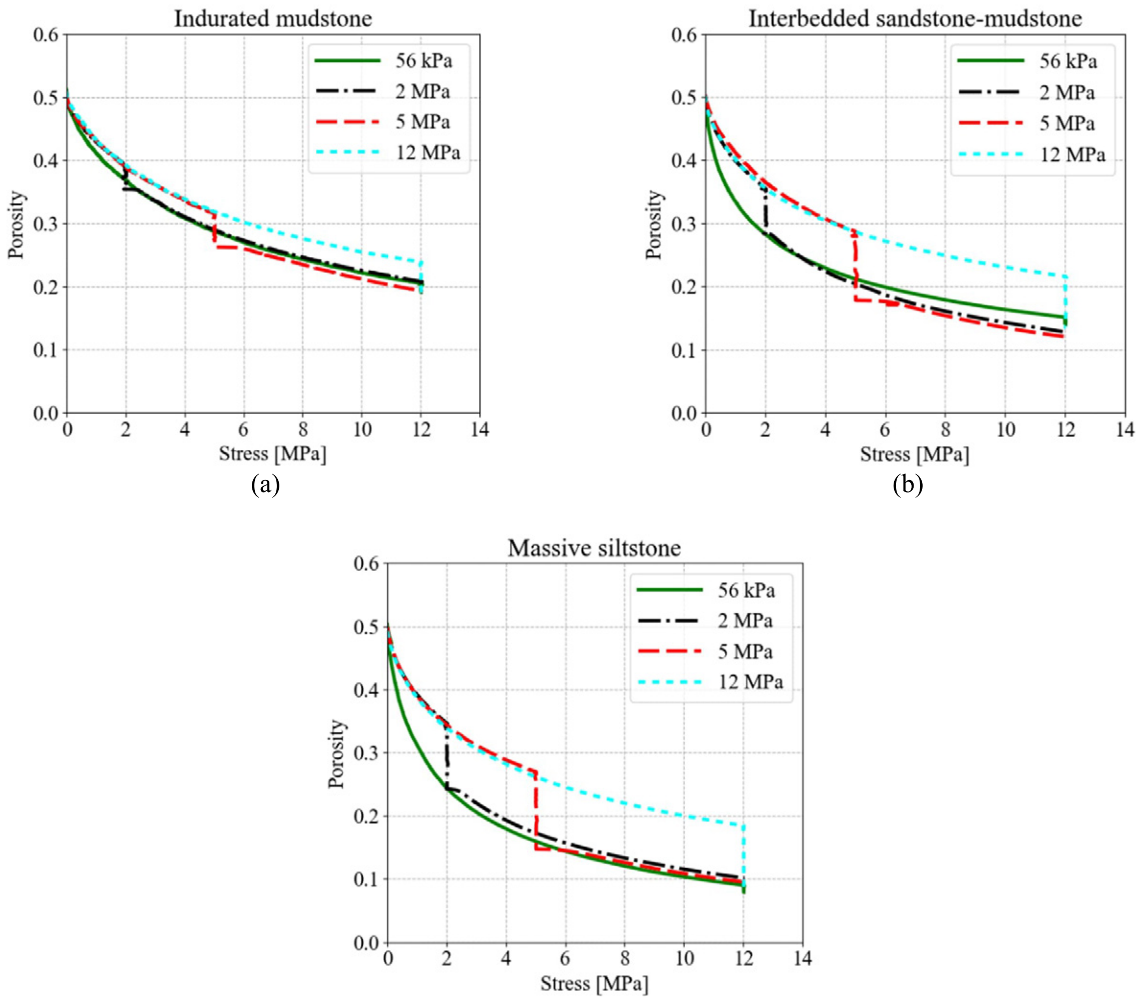

Figure 9 Porosity vs. stress results of specimens for different inundation stresses. (a) indurated mudstone; (b): interbedded sandstone-mudstone; (c): massive siltstone.

The greater collapse potential recorded for the massive siltstone would suggest that it is a weaker or more moisture-sensitive material compared to the other two materials. Indeed, the mean UCS values of 42 MPa, 73 MPa and 157 MPa for the massive siltstone, interbedded sandstone-mudstone, and indurated mudstone confirm this suggestion.

4 DISCUSSION

Figure 11 shows axial strain vs. log(stress) for dry and inundated samples of indurated mudstone, interbedded sandstone-mudstone and massive siltstone. According to Oldecop and Alonso (2001), the granular interactions in a sample subjected to increasing compressive stress starts with particle rearrangement under low-stress levels, and transition through four recognisable stages, denoted as M1 to M4 in Figure 11:

- Zone M1 in Figure 11 corresponds to a particle rearrangement mechanism with negligible particle crushing, and it follows a linear path with stress plotted on a log scale.
- As stress increases, particle crushing becomes an increasingly dominant mechanism. This stage is called clastic yielding and the axial strain vs. log(stress) curve changes from linear to strongly curved with the concavity towards the strain axis. This zone is denoted as M2 in Figure 11.
- In zone M3, particle crushing continues and the granular material structure changes to the new structure in which neighbouring particle sizes are not the same and only the smallest particles will be reduced as stress increases. This stage is called clastic hardening and is characterised by a linear evolution of axial strain vs. log(stress).
- Finally, the axial strain vs. log(stress) becomes non-linear again with upward concavity which indicates the limit for the deformation and crushing of small particles (zone M4 in Figure 11).

It should be noted that it was not possible to obtain a PSD after testing of the sedimentary rocks in this study, since the high clay content resulted in a very cohesive compressed block, of similar strength to the particles themselves. This meant that individual particles could not be separated without a significant likelihood of causing further particle breakage. Therefore, the indicated zones M1 to M4 are based on the definition of compression mechanisms using the shape of the axial strain-log(stress) relationship (see Figure 11). Vertical solid and dashed blue lines are used to show the threshold stresses in dry and inundated conditions, respectively. It can be seen that the threshold stresses between the zones are different for dry and inundated conditions but no clear trend can be identified. Nevertheless, no significant reduction is observed for the indurated mudstone, indicating that the strongest material tested is less sensitive to water.

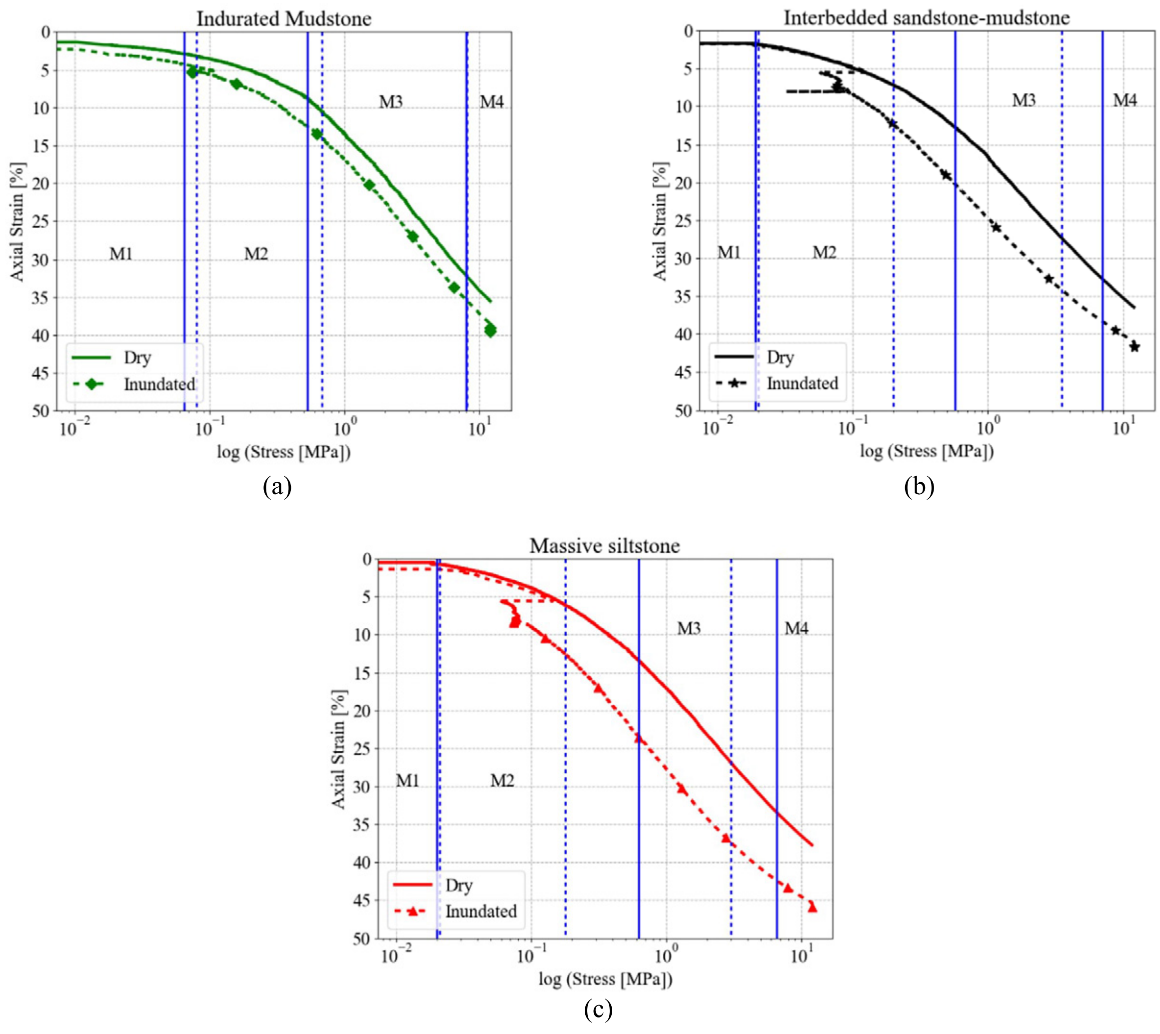

Figure 11 Axial strain vs. log(stress) for different lithologies: (a) indurated mudstone, (b) interbedded sandstone-mudstone, and (c) massive siltstone. The vertical solid and dashed blue lines indicate the threshold stresses in dry and inundated conditions, respectively.

Figure 12 shows the porosity reduction versus stress for samples subjected to dry compression, and the porosity reduction upon inundation at different values of applied stress, for all lithologies considered in this study. All experiments start from the loosest possible state at a very similar porosity of about 0.5, but the porosity of dry specimens under 12 MPa varies with the rock lithology: the strongest material (indurated mudstone) has the highest remaining porosity while the weakest material (massive siltstone) has the lowest one. The same trend is observed for the collapse upon inundation at 12 MPa. Figure 12 also shows that specimens of the same lithology experienced a similar amount of collapse upon inundation, regardless of the stress under which inundation took place. This demonstrates that the collapse upon inundation is a function of lithology and the applied stress plays a negligible role in the response of a specific rock lithology to wetting, especially in the M3 and M4 zones.

Particle rearrangement is the dominant mechanism for the reduction of the porosity of the rock specimen under lower stresses (see Li et al. 2019a). This is the reason why all curves fall in a very narrow band in zone M1 (Figure 11). Then, particle crushing becomes prevalent under intermediate stress levels, and the stronger the rock, the less crushing occurs. Hence, the gap between the compression curves of strong and weak lithologies widens with increasing stress. The dominant mechanism finally changes to filling of pores with rock fragments at higher stress levels, leading to a less compressible material (zone M4). This change of response is more evident for weaker rocks. It should be noted that the dominant mechanism for the compression of material changes gradually and smoothly as stress increases since the specimen particle size distribution is well-graded.

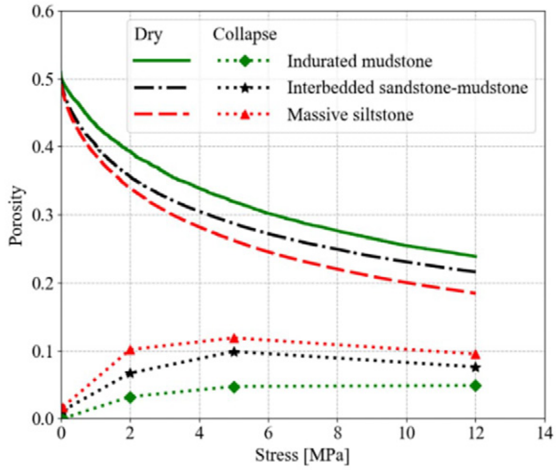

Figure 12 Evolution of porosity vs. stress in dry compression and collapse upon inundation (dotted lines).

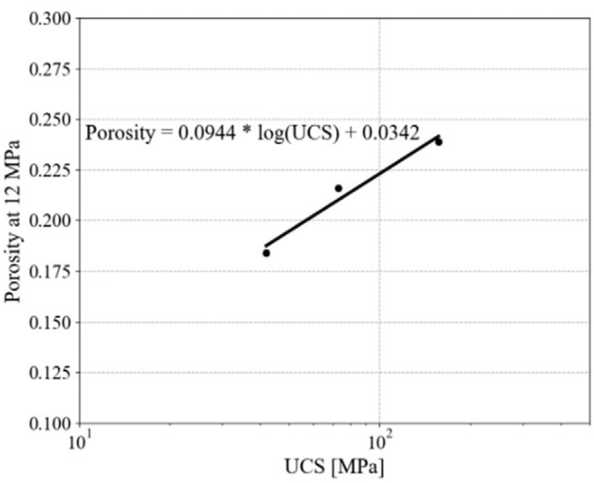

(a)

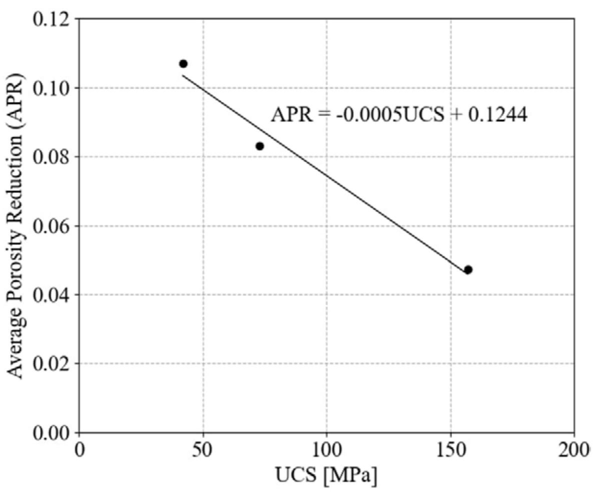

(b)

Figure 13 (a) Evolution of porosity at 12 MPa under dry compression with UCS and (b) average porosity reduction (APR) upon inundation with UCS.

For practical purposes, when studying the feasibility of a UPHES project, it is useful to establish correlations between rock properties that can be easily measured (such as the UCS) and the porosity reduction due to wetting-induced collapse. Figure 13a shows the porosity in each specimen under a compressive stress of 12 MPa (i.e., at the end of dry compression) and Figure 13b shows the average porosity reduction (APR) upon inundation (taken as the average value of porosity reductions at inundation stresses of 2, 5 and 12 MPa) for various lithologies vs. UCS. There is a clear trend that stronger materials undergo less compression for the same loading under dry conditions and collapse less when inundated. Two trendlines are proposed based on the experimental findings of this study but more results (under similar testing conditions) would be required to better validate those trends.

The tests conducted on laboratory-scale specimens provide insight into the magnitude of collapse that might be expected in crushed sedimentary rock of a particular UCS, under a given applied stress, when subjected to inundation. The results are potentially useful in evaluating the likely reduction in porosity that could occur when rubble from mined sedimentary rock is inundated, but a relevant question to pose in the context of a UPHES exploiting abandoned longwall coal mines is how and if these results need to be scaled to account for the dimensions of rocks constituting the goaf (with average maximum block sizes up to around 600 mm, see Figure 1).

To try to answer this question, we consider the results of two dry compression tests carried out in a 560 mm diameter, 475 mm high, heavy-walled oedometer ring, on poorly graded samples of massive siltstone particles, of sizes 19-26 mm and 150-200 mm. The ratio of sample diameter to the maximum particle size is 2.75 in the sample with larger particle sizes. To minimise boundary effects on test results, prepare a homogeneous sample and avoid the formation of large voids at the boundary, particles were placed by hand inside the ring. The results in Figure 14 show that there is no clear effect of particle size on the stress-strain curves, which is consistent with results by Frossard et al. (2012), and they suggest that there is no need to scale the magnitude of collapse measured in the laboratory.

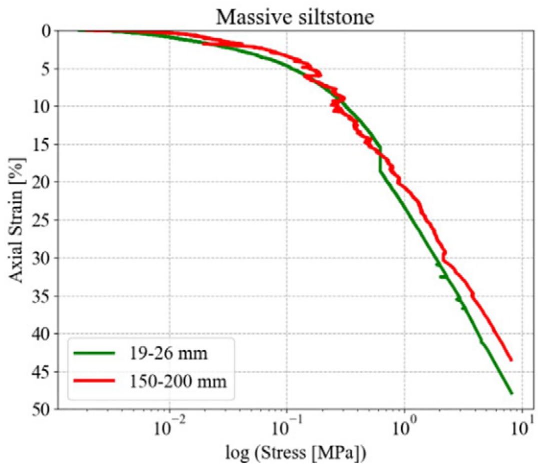

Figure 14 Axial strain vs. log (stress) for dry samples with narrow particle size distributions.

On the other hand, Frossard et al. (2012) observed a scale effect for compression in rockfill particles and derived Equation 1 to scale the stress that would need to be applied to particles of different sizes, to achieve the same compressive strain:

$$\sigma_B = \left(\frac{D_B}{D_A}\right)^{-\frac{3}{m}} \sigma_A \tag{1}$$

In Equation 1, σ_A and σ_B are stresses applied to samples of the same material with characteristic particles sizes D_A and D_B respectively, (where D_A and D_B could be the maximum grain size, mean grain size, or other given characteristic diameter), and m is the Weibull modulus (also called Weibull shape parameter) for some characteristic material strength parameters. The distributions of point load and UCS tests were used to calculate m for the rock lithologies used in this study (see Appendix A).

Equation 1 can be used to scale the dry and inundated stress-strain curves, and to estimate the wetting-induced collapse of full-scale goaf material from laboratory-scale test data, assuming that the particle size distributions have the same shape.

Figure 15 shows the reduced-scale laboratory test results (in green) and predictions for real goaf (in red) for loading under dry and inundated conditions. The collapse upon wetting is estimated by the vertical distance between the two curves. It appears that Equation 1 scales the dry and inundated curves in the same way, so that their relative position remains unchanged, hence predicting that the magnitude of collapse is not particle size dependent. In conclusion, provided that the PSD of the material tested in the lab has the same shape as that of the goaf, the results suggest that it is possible to determine meaningful estimates of the magnitude of collapse in goaf by testing reduced scale samples in the laboratory, without having to scale the results to account for the actual block size of the goaf. It is noted that predicted results are a function of Weibull modulus and the shift from green to red responses in Figure 15 reduces as the Weibull modulus increases.

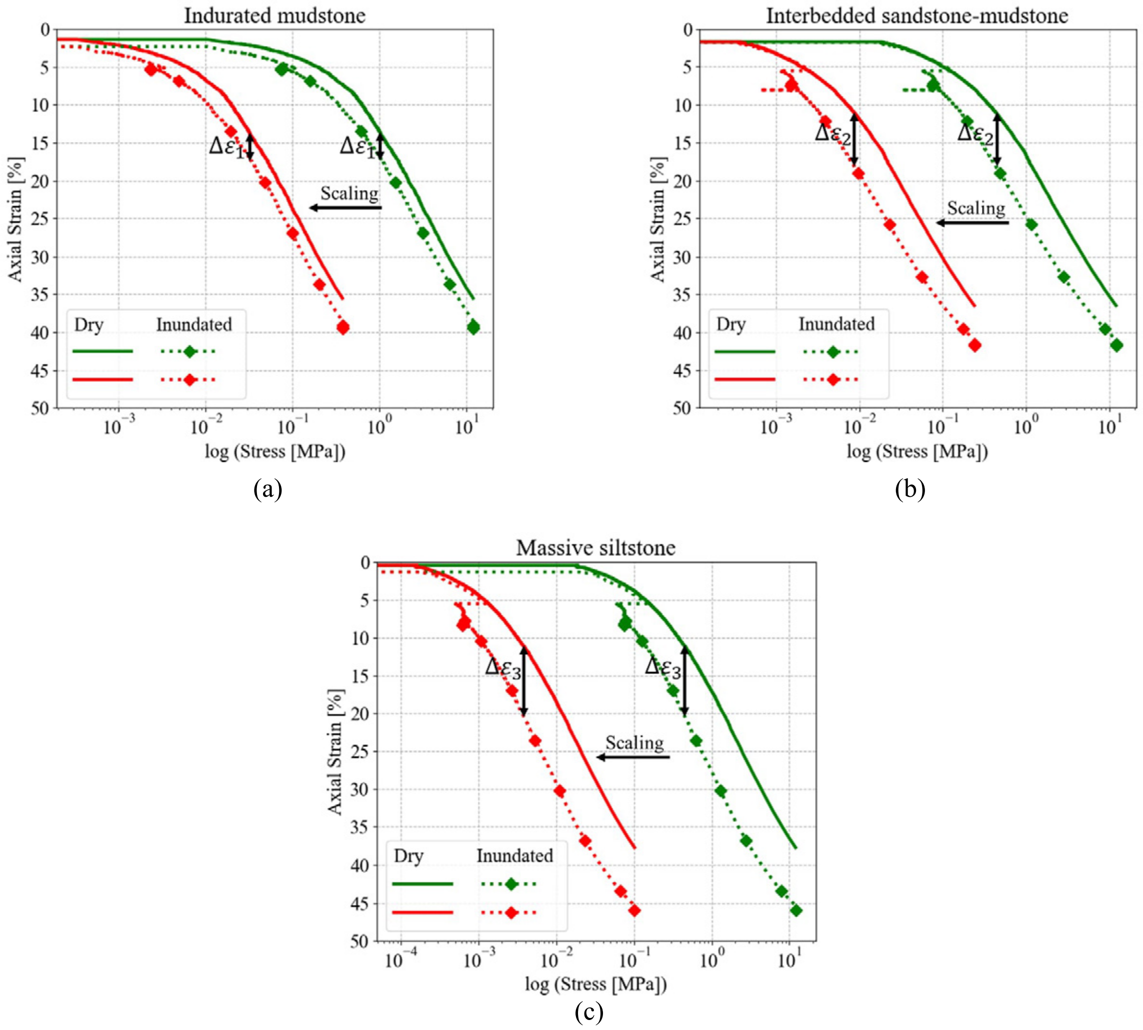

Figure 15 Axial strain vs. log (stress) for dry and inundated samples, where green shows the down-scaled laboratory test results, while red shows the predicted stress under the same stress for real goaf (i.e., 16 times larger PSD): (a) indurated mudstone, (b) interbedded sandstone-mudstone, and (c) massive siltstone.

5 CONCLUSIONS

This paper investigates the mechanical response in 1D compression with wetting-induced collapse of three sedimentary rocks of different material strengths: crushed indurated mudstone, crushed interbedded sandstone-mudstone, and crushed massive siltstone in dry and inundated conditions. Well-graded specimens of dry crushed rock were prepared at the loosest possible state, resulting in a porosity of about 0.5. These were compressed with a strain rate of 1 mm/min until a predetermined inundated stress (ranging from 56 kPa to 12 MPa) was reached. The samples were then inundated under constant load to induce collapse. Subsequently, loading was resumed up to an axial stress of 12 MPa. The following concluding remarks are drawn from this study:

- All sedimentary rock types tested experienced some collapse upon inundation. This finding highlights that wetting-induced collapse is a phenomenon that should not be overlooked or ignored in the design of UPHES facilities.

- The reduction of porosity due to loading and wetting-induced collapse is strongly correlated to the strength of the rock lithology. Some preliminary trendlines were proposed to relate porosity reduction and UCS, but these need to be confirmed with data for more lithologies of different strengths obtained using similar testing conditions. Such trendlines would be very useful to estimate the magnitude of compression and wetting-induced collapse for a given rock of particular strength.
- In the range of 2 to 12 MPa, the stress acting on the specimen when inundation occurs does not affect the consequent magnitude of collapse. This finding is important for the evaluation of UPHES in goafed rock since it is very difficult to estimate the stress the goaf material is under.
- This study did not separately consider the water sensitivity of the different lithologies tested, but instead, implicitly captures the general tendency that sensitivity to water increases as the UCS decreases. Several results from the literature show little influence of PSD on the dry compression curves of crushed rock, provided that the overall shape of the PSD does not change. Consequently, provided that the PSD of the material tested in the laboratory has a similar shape as that of the goaf, the results suggest that it is possible to estimate the magnitude of collapse in goaf using reduced scale tests in the laboratory, without having to scale the results to account for the actual block size of the goaf. This same conclusion can be drawn when employing a scaling law established by Frossard et al. (2012) for rockfill.

ACKNOWLEDGEMENT

This research was a component of a larger study conducted by Banpu Energy Australia Pty Ltd into the feasibility of using longwall goafs as lower reservoirs for pumped hydroelectric schemes. Banpu received funding from the Australian Renewable Energy Agency (ARENA) of the Australian Government as part of ARENA's Advancing Renewables Program as well as the NSW Emerging Energy Program (EEP). The assistance of Banpu Energy staff, in particular Matthew Fellowes, and access to Banpu Energy facilities are greatly appreciated.

CRediT authorship contribution statement

Mehrdad Ahmadi: Formal Analysis, Writing – original draft. **Stephen Fityus:** Funding acquisition, Methodology, Writing – review & editing. **Klaus Thoeni:** Funding acquisition, Methodology, Project administration, Writing – review & editing. **Ross Seedsman:** Conceptualisation, Writing – review & editing. **Anna Giacomini:** Funding acquisition, Writing – review & editing. **Olivier Buzzi:** Funding acquisition, Methodology, Writing – review & editing.

REFERENCES

Bagde MN, Raina AK, Chakraborty AK, Jethwa JL (2002) Rock mass characterization by fractal dimension. Eng Geol 63:141–155. https://doi.org/10.1016/S0013-7952(01)00078-3

Fan J, Xie H, Chen J, et al (2020) Preliminary feasibility analysis of a hybrid pumped-hydro energy storage system using abandoned coal mine goafs. Appl Energy 258:114007. https://doi.org/10.1016/j.apenergy.2019.114007

Fityus S, Hancock G, Wells T (2008) Geotechnical characteristics of coal mine spoil. Aust Geomech J 43:13–22

Frossard E, Hu W, Dano C, Hicher PY (2012) Rockfill shear strength evaluation: A rational method based on size effects. Geotechnique 62:415–427. https://doi.org/10.1680/geot.10.P.079

Hunter G, Fell R (2003) Rockfill Modulus and Settlement of Concrete Face Rockfill Dams. J Geotech Geoenvironmental Eng 129:909–917. https://doi.org/10.1061/(asce)1090-0241(2003)129:10(909)

ISRM (1979) Suggested Methods for Determining Uniaxial Compressive Strength and Deformability of Rock Materials. Int J Rock Mech Min Sci 16:137–140

Jain KR, Edraki M, McIntyre N (2021) Controls of Wetting and Drying Cycles on Salt Leaching from Coal Mine Spoils. Water Air Soil Pollut 232:472. https://doi.org/10.1007/s11270-021-05422-7

Jiang D, Chen S, Liu W, et al (2021) Underground Hydro-Pumped Energy Storage Using Coal Mine Goafs: System Performance Analysis and a Case Study for China. Front Earth Sci 9:1–15. https://doi.org/10.3389/feart.2021.760464

Karacan CÖ (2010a) Prediction of porosity and permeability of caved zone in longwall gobs. Transp Porous Media 82:413–439. https://doi.org/10.1007/s11242-009-9437-7

Karacan CÖ (2010b) A new method to calculate permeability of gob for air leakage calculations and for improvements in methane control. Proc 13th US/North Am Mine Vent Symp

Karem WA, Kalinski ME, Hancher DE (2007) Settlement of Mine Spoil Fill from Water Infiltration: Case Study in Eastern Kentucky. J Perform Constr Facil 21:345–350. https://doi.org/10.1061/(asce)0887-3828(2007)21:5(345)

Khalili A, Kromp K (1991) Statistical properties of Weibull estimators. J Mater Sci 26:6741–6752

Li B, Liang Y, Zhang L, Zou Q (2019a) Experimental investigation on compaction characteristics and permeability evolution of broken coal. Int J Rock Mech Min Sci 118:63–76. https://doi.org/10.1016/j.ijrmms.2019.04.001

Li M, Zhang J, Gao R (2016) Compression characteristics of solid wastes as backfill materials. Adv Mater Sci Eng 2016:1–7. https://doi.org/10.1155/2016/2496194

Li M, Zhang J, Song W, Germain D (2019b) Recycling of crushed waste rock as backfilling material in coal mine: effects of particle size on compaction behaviours. Environ Sci Pollut Res 26:8789–8797. https://doi.org/10.1007/s11356-019-04379-9

Li M, Zhang J, Sun K, Zhang S (2018) Influence of lateral loading on compaction characteristics of crushed waste rock used for backfilling. Minerals 8:552. https://doi.org/10.3390/min8120552

Li M, Zhang J, Wu Z, et al (2019c) An experimental study of the influence of lithology on compaction behaviour of broken waste rock in coal mine backfill. R Soc Open Sci 6:1–12. https://doi.org/10.1098/rsos.182205

Liu A, Liu S, Wang G, Elsworth D (2020) Continuous Compaction and Permeability Evolution in Longwall Gob Materials. Rock Mech Rock Eng 53:5489–5510. https://doi.org/10.1007/s00603-020-02222-z

Ma D, Bai H, Miao X, et al (2016) Compaction and seepage properties of crushed limestone particle mixture: an experimental investigation for Ordovician karst collapse pillar groundwater inrush. Environ Earth Sci 75:1–14. https://doi.org/10.1007/s12665-015-4799-3

Neves EM das, Pinto AV (1988) Modelling collapse on rockfill dams. Comput Geotech 6:131–153

Oldecop LA, Alonso EE (2001) A model for rockfill ll compressibility. Geotechnique 51:127–139

Pappas MD, Mark C (1993) Behavior of Simulated Longwall Gob Material. RI 9458

Salmi EF, Sellers EJ (2021) A review of the methods to incorporate the geological and geotechnical characteristics of rock masses in blastability assessments for selective blast design. Eng Geol 281:105970. https://doi.org/10.1016/j.enggeo.2020.105970

Standards Australia (2013) Rock strength test – determination of uniaxial compressive strength – rock strength less than 50 MPa (AS 4133.4.2.2-2013). Retrieved from SAI Glob

Standards Australia (2009) Methods of Testing Rocks for Engineering Purposes – Rock Strength Tests – Determination of Deformability of Rock Materials in Uniaxial Compression – Strengths of 50 MPa and Greater (AS 4133.4.3.1). Retrieved from SAI Glob

Tabibnejad A, Heshmati A, Salehzadeh H, Tabatabaei SH (2015) Effect of gradation curve and dry density on collapse deformation behavior of a rockfill material. KSCE J Civ Eng 19:631–640. https://doi.org/10.1007/s12205-013-0682-5

Tiryakioğlu M, Hudak D (2007) On estimating Weibull modulus by the linear regression method. J Mater Sci 42:10173–10179. https://doi.org/10.1007/s10853-007-2060-5

Wang L, Kong H, Karakus M (2020) Hazard assessment of groundwater inrush in crushed rock mass: An experimental investigation of mass-loss-induced change of fluid flow behavior. Eng Geol 277:105812. https://doi.org/10.1016/j.enggeo.2020.105812

Xu J, Pu H, Chen J, Sha Z (2021) Experimental Study on Sand Inrush Hazard of Water-Sand Two-Phase Flow in Broken Rock Mass. Geofluids 2021:1–9. https://doi.org/10.1155/2021/5542440

Yu B, Chen Z, Ding Q, Wang L (2016) Non-Darcy flow seepage characteristics of saturated broken rocks under compression with lateral constraint. Int J Min Sci Technol 26:1145–1151. https://doi.org/10.1016/j.ijmst.2016.09.025

Zhang C, Bai Q, Zhu C (2022) A methodology for determining the size distribution of broken rock masses in longwall mining goaf. Geomech Geophys Geo-Energy Geo-Resources 8:113. https://doi.org/10.1007/s40948-022-00418-x

Zhou X, Chi S, Jia Y, Shao X (2020) A new wetting deformation simulation method based on changes in mechanical properties. Comput Geotech 117:103261. https://doi.org/10.1016/j.compgeo.2019.103261

APPENDIX A

According to Tiryakioğlu and Hudak (2007) the Weibull modulus m can be estimated using Equation A1:

$$\ln[-\ln(1-P)] = m\ln(\sigma) - m\ln(\sigma_0) \tag{A1}$$

where P is the probability of failure at a stress σ and σ_0 is the scale parameter. Therefore, m is the slope of a line with the intercept of $-m\ln(\sigma_0)$. The probability parameter P can be determined using Equation A2:

$$P = \frac{i-a}{n+b} \tag{A2}$$

where i and n are the rank of the data in an ascending list of available data and the size of the list, respectively. a and b are probability estimators and they should be adopted from the following range $0 \leq a \leq 0.5$ and $0 \leq b \leq 1.0$. Various combinations of a and b can be used which subsequently influence P and m. In this study, $a = 0.5$ and $b = 0$ are used as these values are commonly used in the literature, see e.g. Khalili and Kromp (1991).

The UCS and point load test (PLT) data are used in Figure A1. Very similar m is achieved for the indurated mudstone using both UCS and PLT results indicating that both UCS and PLT can be used in determining m. Due to the limited availability of the material sourced from underground goaf, the UCS results provided by the mine site are used in estimating the m value for interbedded sandstone-mudstone. However, PLT results were used for the massive siltstone. According to Figure A1, m is 2.68, 2.39 and 1.96 for indurated mudstone, interbedded sandstone-mudstone and massive siltstone, respectively. It should be noted that interbedded sandstone-mudstone includes 1/3 mudstone and 2/3 sandstone, so the weighted average of m values from Figures A1b-c is used for this lithology.

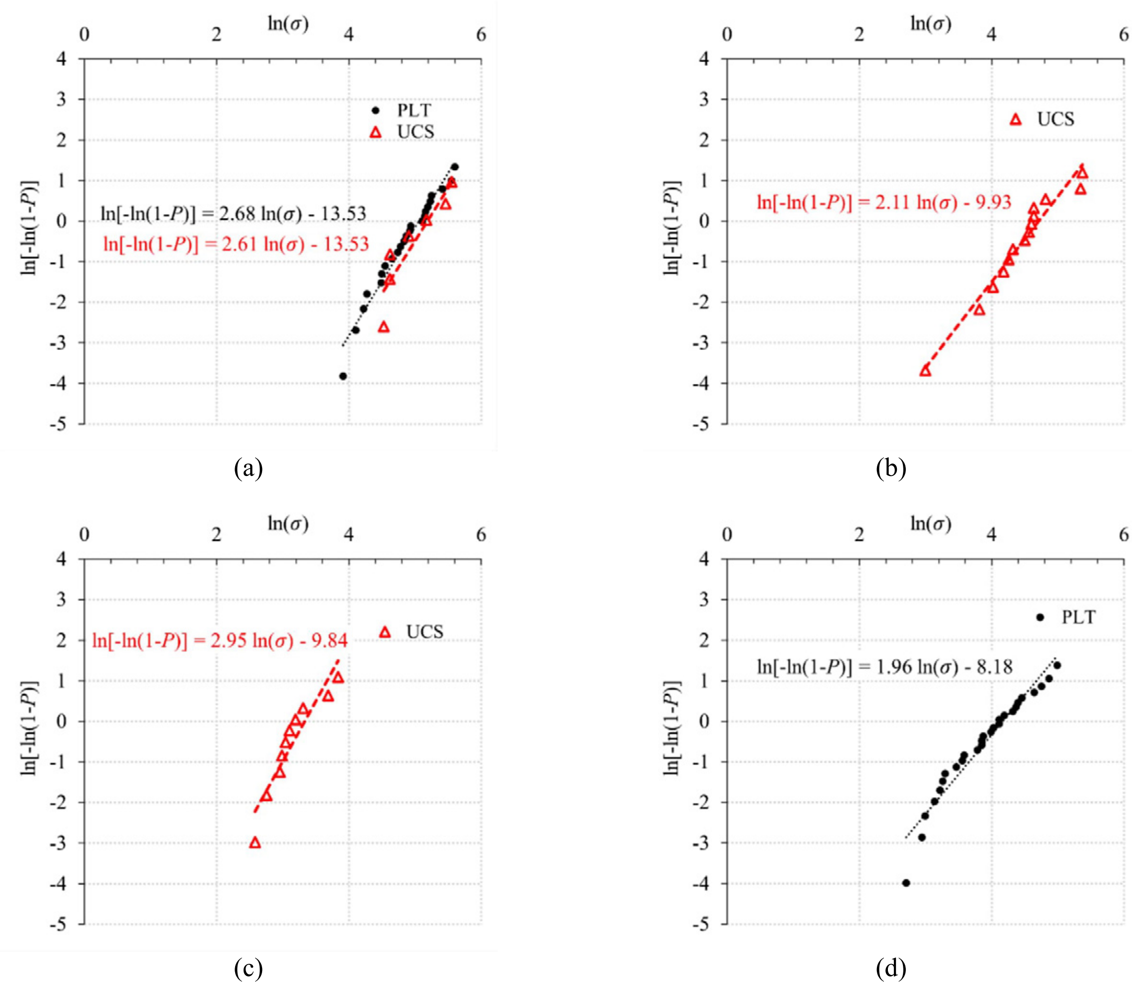

Figure A1 ln[-ln(1-P)] vs. ln(σ) for different lithologies: (a) indurated mudstone, (b) sandstone of indurated sandstone-mudstone, (c) mudstone of indurated sandstone-mudstone, and (d) massive siltstone.